Published in final edited form as:
Comp Biochem Physiol A Mol Integr Physiol. 2010 September ; 157(1): 55–62. doi:10.1016/j.cbpa.2010.05.002.

Physiological and pharmacological characterization of the larval *Anopheles albimanus* rectum supports a change in protein distribution and/or function in varying salinities

Kristin E. Smith[a], **Steven L. Raymond**[a], **Micheala L. Valenti**[a], **Peter J.S. Smith**[b], and **Paul J. Linser**[b,a*]

[a]The Whitney Laboratory for Marine Bioscience, University of Florida, 9505 OceanShore Boulevard, St Augustine, FL 32080, USA

[b]BioCurrents Research Center, Marine Biological Laboratory, 7 MBL St., Woods Hole, MA 02543, USA

Abstract

Ion regulation is a biological process crucial to the survival of mosquito larvae and a major organ responsible for this regulation is the rectum. The recta of anopheline larvae are distinct from other subfamilies of mosquitoes in several ways, yet have not yet been characterized extensively. Here we characterize the two major cell types of the anopheline rectum, DAR and non-DAR cells, using histological, physiological, and pharmacological analyses. Proton flux was measured at the basal membrane of 2%- and 50%-artificial sea water-reared *An. albimanus* larvae using self-referencing ion-selective microelectrodes, and the two cell types were found to differ in basal membrane proton flux. Additionally, differences in the response of that flux to pharmacological inhibitors in larvae reared in 2% versus 50% ASW indicate changes in protein function between the two rearing conditions. Finally, histological analyses suggest that the non-DAR cells are structurally suited for mediating ion transport. These data support a model of rectal ion regulation in which the non-DAR cells have a resorptive function in freshwater-reared larvae and a secretive function in saline water-reared larvae. In this way, anopheline larvae may adapt to varying salinities.

Keywords

DAR; ion regulation; ISMs; mosquito; self-referencing

1. Introduction

Mosquitoes (Diptera: Culicidae) are hosts to a number of mammalian pathogens including parasites, bacteria, viruses, and fungi. The worst of all vector-borne diseases is malaria; it is one of the top three killers among communicable diseases, infecting 500 million people worldwide, and killing at least two million people each year (World Health Report 1996; Sachs and Malaney 2002). All of the world's human malaria, as well as many other deadly diseases, is vectored by the anopheline subfamily of mosquitoes. In order to control these devastating

*Corresponding author: Tel: 904-461-4036; Fax: 904-467-4008; *pjl@whitney.ufl.edu*.

diseases it is critical to understand the processes necessary for vector survival. This knowledge can foster the development of novel techniques to reduce the vector population both specifically and safely. Mosquito larvae, like all aquatic organisms, must adapt to an environment which can change drastically in ionic composition and salinity. Adaptation to these varying conditions requires a highly developed system for the regulation of ions, and a major organ responsible for this regulation is the rectum. The rectum modifies urine prior to excretion based on the ionic needs of the larva by resorbing essential ions and nutrients and/or excreting excess salts and waste products. The recta of several culicine larvae have been extensively studied and are structurally distinct between freshwater and saline-tolerant species (Meredith and Phillips 1973). Freshwater species have a structurally and functionally uniform rectum which resorbs water and ions from the primary urine. Saline-tolerant species have a structurally segmented rectum divided into an anterior rectum (AR), which is similar in function to the recta of fresh water species, and a posterior rectum (PR), which secretes a hyperosmotic urine. Although to date, the majority of work on larval ion regulation has focused on the culicine subfamily, we and others have shown that the recta of anopheline larvae differ from that of both freshwater and saline-tolerant culicine species in structure (Bradley 1987a; Bradley 1987b; Smith K.E. et al. 2007) and in regulation of protein expression (Smith et al. 2008).

The recta of anopheline larvae are similarly structured regardless of saline tolerance and consist of DAR[1] cells (dorsal anterior rectal cells) and non-DAR cells (anterior ventral cells and all posterior cells) (Smith, K. E. et al. 2007; Smith et al. 2008). Although all anopheline species examined to date possess recta which resemble this structure (Smith et al. 2008), the distribution of at least one ion-regulatory protein, Na^+/K^+-ATPase, changes depending on the salinity of the external milieu. Primary distribution of Na^+/K^+-ATPase shifts from the non-DAR cells in larvae reared in freshwater, to the DAR cells in larvae reared in saline water (≥30% artificial sea water, ASW) (Smith et al. 2008). As a result, the rearing of larvae in different salinities elicits different patterns of protein expression in the rectal regions, and may result in a change in overall function of the rectum. In this way, larvae can survive in freshwater by resorbing essential ions and nutrients, and in saline water (in the case of saline-tolerant species) by generating a hyperosmotic urine, while using the same rectal cell types.

We hypothesize that anopheline larvae shift protein distribution patterns in their rectal regions to activate the non-DAR cells, which comprise approximately 75% of the cells of the rectum, to either resorb or secrete ions based on larval osmotic requirements. By expressing different combinations of ion-regulatory proteins, the rectal cells may favor the function of one protein over another. Many ion-regulatory transporters can activate other proteins by generating favorable electrochemical gradients across a membrane. Often these gradients are generated by the uneven distribution of protons (H^+) across a membrane, and indeed many proteins facilitate the transport of protons across insect membranes including V-ATPase (Wieczorek et al. 1991), Na^+/H^+-exchangers (Pullikuth et al. 2006), Na^+/H^+ antiporters (Padan et al. 2001; Rheault et al. 2007), and K^+/H^+ exchangers (Harvey and Nedergaard 1964).

Here we characterize the cells of the anopheline rectum using histological, physiological, and pharmacological methods. We report proton flux at the basal membrane of the DAR and non-DAR cells of freshwater- and saline water-reared *An. albimanus* larvae using self referencing ion selective microelectrodes (ISMs) (Smith, P. J. et al., 2007) and the effects of pharmacological inhibition of that flux. Our data indicate that there are distinct differences between the rectal DAR and non-DAR areas in structure, the direction of net proton flux, and in the proteins mediating this flux. Additionally, there are distinct differences in the roles of several of these proteins in mediating proton flux between larvae reared in 2% versus 50% ASW. We use these results, together with previous immunohistochemical data, to generate a putative model for ion control in the larval anopheline rectum and discuss how this model relates to our previous hypothesis regarding the role of the anopheline rectum in ion regulation.

2. Materials and Methods

2. 1. Artificial Sea Water (ASW)

100% artificial sea water (ASW) in mmol L^{-1}: 420 NaCl; 9 KCl; 12 $CaCl_2$; 23 $MgCl_2$; 26 $MgSO_4$; and 2 $NaHCO_3$ in milli-Q water (Millipore, Billerica, MA, USA), pH 8.1, osmolarity: 860 mosmol L^{-1} as measured using a 5500 vapor pressure osmometer (Wescor, Logan, UT, USA). All dilutions of the 100% ASW stock were made using milli-Q water.

2.2. Model organism

Anopheles albimanus (Weidemann) and *Anopheles gambiae* (SS G3) were hatched from eggs supplied by MR4 (The Malaria Research and Reference Reagents Resource Center) at the Centers for Disease Control and Prevention in Atlanta, GA, USA (http://www.malaria.atcc.org) and reared as described in the supplier manual (www2.ncid.cdc.gov/vector/vector.html). Larvae were hatched and reared in either 2% ASW or 50% ASW in milli-Q water at a density of approximately 100 larvae per 200 mL water and fed every other day with a dusting of ground TetraMin™ fish flakes.

2.3. Rectal cell histology and cytology

Early fourth-instar *An. gambiae* larvae were injected in the hemocoel with 2.5% gluteraldehyde in 0.1M phosphate buffer and fixed >24 hours in the same solution. The tissue was rinsed five times in PBS, and post-fixed in 1% osmium tetroxide, in the same buffer, for one hour at 4 ° C. Samples were subsequently rinsed twice with distilled water for five min each and dehydrated in an ethanol series (25% for five min, 50% for five min, 70%, 85%, and 95% three times each for ten min, and 100% five times each for ten min), culminating in two changes of propylene oxide with a waiting period of 15 min after each change. The samples were then placed in Epon (Embed-812, Electron Microscopy Sciences, Hatfield, PA, USA) mixture/ propylene oxide (1/1) for one hour at room temperature, followed by incubation in Epon mixture/propylene oxide (3:1) overnight at 60 °C. Samples were then incubated in two changes of pure Epon for two hours each and embedded by placing in molds with fresh Epon mixture polymerizing at 60 °C for 48 h. Semithin (0.5–1.5 μm) sections were cut with a diamond knife (Micro Star Tech, Huntsville, TX, USA) on a Sorvall Porter-Blum ultramicrotome (MT-2) and stained with Richard's stain for approximately 4 min at 94 °C. Richard's stain was prepared by mixing equal volumes of 1% methylene blue in 1% sodium borate together with 1% Azure II in milli-Q water, and filtered prior to staining. Transmission electronmicroscopy (TEM) was performed on ultrathin sections mounted on nickel grids and post-stained with lead citrate and uranyl acetate by standard methods (e.g. Richards et al., 1977).

2.4. Physiology preparation

Late third-instar *An. albimanus* larvae were anesthetized on ice for 30 min prior to dissection in artificial hemolymph solution (modified from Clark et al. 1999; in mmol L^{-1}: 42.5 NaCl, 3.0 KCl, 0.6 $MgSO_4$, 5.0 $CaCl_2$, 5.0 $NaHCO_3$, 5.0 succinate, 5.0 malate, 5.0 L-proline, 9.1 L-glutamine, 8.7 L-histidine, 3.3 L-arginine, 10.0 glucose, 5.0 HEPES in milli-Q water, pH 7.1; osmolarity adjusted to 300 mosmol L^{-1} with D-mannitol). Larvae were pinned to a sylgard coated petri dish through the head, and the exoskeleton surrounding the ileum, Malpighian tubules and rectum were removed. Exoskeleton surrounding the anterior extreme of the larva was left intact. Malpighian tubules were either removed or pinned away from the rectum. The rectum was immobilized by adhering one side to a poly-lysine-coated coverslip which had been immersed in a 2.0 mg mL^{-1} poly-lysine solution in milli-Q water for 30 minutes.

2.5. Proton flux at basal membrane of DAR and non-DAR cells

Proton gradients were measured at the basal membrane of *An. albimanus* recta using self-referencing ISMs (see Smith et al. 1999, 2007 and Messerli et al. 2006). ISMs were made from 1.5 mm diameter borosilicate thin-wall glass capillary tubes pulled to a tip diameter of approximately 2-3 μm (TW150- 6, WPI, Sarasota, FL, USA) using a Sutter P-97 micropipette puller (Sutter instruments Inc., Novato, CA, USA) and salinized as described in Smith, P.J. et al (2007). The micropipettes were then backfilled with 100 mmol L^{-1} KCl, 10 mmol L^{-1} HEPES, pH 7.4 and tip filled with a 30 μm column of H^+ ionophore 1 in cocktail A (Selectophore (Fluka) Sigma-Aldrich). When in use the ISM was translated between two poles within the ion gradient. The resulting voltages depended on the ion activity at each pole of translation. Calculating the differential of the two values minimized the impact of circuit drift and subtracted out background values and other voltages constant to both poles of measurement (see Smith, P. J. et al., 2007 and Messerli et al., 2006). Motion controllers, stepper motors, amplifiers and software were products of the BioCurrents Research Center (Woods Hole, MA, USA).

ISMs were calibrated against known pH values allowing the differential voltages to be converted to a change in concentration which can then be converted to a flux value through Fick's 1st Equation (see below). The ISM output was tested against all pharmacological agents to ensure that there was no interference with the calibration slope or response.

Proton flux was measured approximately 5-10 μm from the membrane beginning at the rectumileum junction and stopping when the end of the rectum was reached. Measurements were taken in 50 μm increments at positions along the anterior-posterior axis of the rectum. Reported measurements for each point along the rectum reflect an average of recordings taken over five minutes at 1000 samples per second, with the first 30% sampled before and after probe excursion being discarded. A proton flux was considered outwardly directed, or an efflux, if the probe detected higher proton activity closest to the membrane. By contrast, an inwardly directed proton flux, or influx, was considered if the probe detected higher proton activity furthest from the membrane. Seven biological replicates were performed.

Because the DAR cells are not visibly discernable from non-DAR cells using a dissecting microscope, preparations were post-stained with rhodamine 123 (Molecular Probes®, Invitrogen, Eugene, OR, USA) following proton flux measurements and imaged using an Axio Observer Z1 microscope (Carl Zeiss Inc., Thornwood, NY, USA) and an AxioCam MRc camera (Carl Zeiss Inc.). The fluorescent staining allowed for the identification of the DAR/non-DAR boundary (see Fig. 2a).

Data was analyzed in Microsoft Excel and graphs were generated using Graphpad Prism 3.0 graphing software (La Jolla, CA, USA). To determine the average DAR and non-DAR proton flux (Fig. 2c), all flux measurements taken from the DAR cells or non-DAR cells of a single preparation were first averaged. Averaged values for all like measurements (all DAR cell measurements or all non-DAR cell measurements) were then averaged and used as raw data for statistical analysis. Statistical significance was determined for all data in Microsoft Excel using a paired t-test and reported as two-tailed P-values.

2.6. Flux (J) Calculations

Ion fluxes (J) were calculated using the following equation:

$$J = D * \frac{C_{av} * 10^{\frac{dv}{slope}} - C_{av}}{\Delta x}$$

Where 'D' is the proton diffusion coefficient ($9.31*10^{-5}$ cm^2 s^{-1}), 'Cav' is the background hemolymph proton concentration (mol cm^{-2}), 'dV' is the voltage difference between the near and far positions (mV), 'Δx' is the probe excursion distance ($2*10^{-3}$ cm_2), and 'slope' is the experimentally determined slope for each probe.

To correct for the buffering capacity of water, bicarbonate, and histidine found in artificial hemolymph, the following equation was used:

$$J_{Htotal} = J_{Hmeasured} * (1 + x_i + \ldots + x_n)$$

The correction factor, 'x_i', is the ratio of proton bound buffer flux to free proton flux and is calculated using the following equation (Messerli et al., 2006) for each buffer (B) present:

$$x_i = \frac{D_B}{D_{H+}} * [B] * \frac{Ka}{(Ka + [H^+])^2}$$

Where '[B]' is the buffer concentration, '$[H^+]$' is the proton concentration, and 'Ka' is the acid constant of the buffer.

2.7. Pharmacology

To determine the effects of pharmacological inhibitors on proton flux, a single point of stable proton efflux in the DAR cells, or influx in the non-DAR cells, was chosen for each preparation. The flux was considered stable if it remained relatively constant over a ten minute period. Measurements were recorded as described above for a period of ten minutes prior to, and ten minutes following, addition of a pharmacological inhibitor.

Concanamycin A (10^{-3} mol L^{-1}; A.G. Scientific Inc., San Diego, CA, USA) and DIDS (10^{-3} mol L^{-1}; Sigma-Aldrich Corp., St. Louis, MO, USA) were prepared in DMSO and added to the preparation at a final concentration of 10^{-6} mol L^{-1}. Methazolamide (0.1 mol L^{-1}; Sigma-Aldrich) was prepared in DMSO, diluted with artificial hemolymph to 10^{-3} mol L^{-1}, and added to the preparation at a final concentration of 10^{-4} mol L^{-1}. All reported results represent an average of $n \geq 5$ preparations. Results were reported as a ratio of flux after treatment, to flux before treatment with a pharmacological inhibitor.

Data were analyzed in Microsoft Excel and graphs were generated using Graphpad Prism 3.0 graphing software. For each bar, a value of "1", for DAR cell flux, or "-1", for non-DAR cell flux, indicates no change in proton flux following addition of inhibitor. A value greater than "1", for DAR cell flux, indicates an increase in proton efflux, whereas a value less than "-1", for non-DAR cell flux, indicates an increase in proton influx. A value less than "1", for DAR cell flux, indicates a decrease in proton efflux, whereas a value greater than "-1", for non-DAR cell flux, indicates a decrease in proton influx. Statistical significance was determined for all data (comparing flux before, to flux after inhibitor) in Microsoft Excel using a paired t-test and reported as two-tailed P-values.

Additionally, the effects of each inhibitor were compared between cell types and rearing conditions to determine statistical significance. For each inhibitor, the ratios of flux after treatment, to flux before treatment with a pharmacological inhibitor for each preparation were used as raw data. A one-way anova with a Tukey post-hoc test was performed to determine if the effect of an inhibitor significantly differed between cell types and/or rearing salinity.

3. Results

3.1. Histology of anopheline rectal cells

Richard's stain was used to post-stain semi-thin (1.5 μm) sections of fourth-instar *An. gambiae* recta (Fig. 1a and b). Two cell types were clearly distinguishable; one type appeared to be larger and possess an apical striated border that extended approximately 30% into the cell. This cell type comprised approximately 75% of the rectum and was predicted to represent the non-DAR cells. The other cell type appeared to be thinner and lack a striated border. This cell type occupied approximately 50% of the anterior extreme of the rectum, corresponding to 25% of the whole rectum and was predicted to represent the DAR cells. Both cell types were bordered on the apical side by a thin layer of cuticle termed the intima which separated the food bolus from the epithelial cells and on the basal side by circumferential muscles.

DAR and non-DAR cells were also distinguishable using electron microscopy (Fig. 1c). Ultrastructurally, the apical membrane of the non-DAR cells was elaborated in the form of apical lamellae which extended approximately 30% into the cell and corresponded to the striated border detected using light microscopy. The remainder of the cell was comprised of a dense network of basal infoldings which stretched from the basal membrane to the space occupied by apical lamellae. By contrast, the DAR cells possessed apical lamellae which extended a much shorter distance into the cell, with the majority of the cell being occupied by basal infoldings. As seen using light microscopy, both cell types were bordered on the apical side by a thin layer of cuticle and on the basal side by circumferential muscles. The DAR and non-DAR cells were separated by a thin junctional cell as seen separating the AR and PR of saline-tolerant culicines (Meredith and Phillips, 1973). Similar histological and cytological details are evident in 2% ASW-reared *An. albimanus* (K.E. Smith, unpublished data).

3.2. Proton flux in rectum

Proton flux was determined at the basal membrane of the DAR and non-DAR cells of intact *An. albimanus* larvae reared in either 2% or 50% ASW using ISMs (Fig. 2). Because DAR and non-DAR cell types cannot be distinguished with a dissecting microscope, measurements were taken along the anterior-posterior axis of one side of the rectum and preparations were post-stained with rhodamine 123 to visualize DAR and non-DAR cell types (Fig. 2a). Proton flux was measured at points approximately 5-10 μm from the membrane in 50 μm increments along the anterior-posterior axis of the rectum (Fig. 2b).

In all larvae a significant proton efflux was observed averaging 1.3×10^{-7} mol cm^{-2} s^{-1} in the region of the DAR cells. Although this efflux was consistent among all larvae, the magnitude of the flux varied greatly between larvae ranging from 1.38×10^{-8} to 3.27×10^{-7} mol cm^{-2} s^{-1}. As the probe neared the DAR/non-DAR boundary, the proton flux decreased significantly and fluctuated between an influx and efflux, averaging 9.6×10^{-9} mol cm^{-2} s^{-1}. Again the magnitude of this flux varied between larvae, but in each individual larva, a trend was noted in which DAR cells exhibited a large proton efflux that decreased considerably at the DAR/non-DAR cell boundary, and often reversed direction in the non-DAR cells (Fig. 2b).

3.3. Pharmacology

To determine the proteins involved in proton flux at the basal membrane of the DAR and non-DAR cells, the effects of concanamycin A, methazolamide and DIDS were evaluated at a single point of proton efflux at the DAR cells and influx at the non-DAR cells (Fig. 3). Concanamycin A is a specific inhibitor of the proton pump, V-ATPase; methazolamide is a specific inhibitor of carbonic anhydrase (CA), a known marker for DAR cells and an enzyme which catalyzes the production of protons and bicarbonate within a cell; DIDS (4,4′-Diisothiocyanatostilbene-2,2′-disulfonic acid Disodium salt) is a specific inhibitor of anion exchange and is effective against bicarbonate transporters, proteins which frequently work in synergy with CAs (McMurtrie et al. 2004). For each inhibitor $n \geq 5$ larvae were examined.

Concanamycin A at a concentration of 10^{-6} mol L^{-1} significantly decreased DAR cell proton efflux in larvae reared in both 2% (P-value < 0.01) and 50% (P-value < 0.05) ASW.

Concanamycin A had no significant effect on non-DAR cell proton influx in 2% or 50% ASW reared larvae at the concentration used. The effect of Concanamycin A on the non-DAR cells of larvae reared in 2% ASW differed significantly from that of the DAR cells of larvae reared in both 2% ASW (P-value < 0.001) and 50% ASW (P-value < 0.05).

Methazolamide at a concentration of 10^{-4} mol L^{-1} significantly decreased DAR cell proton efflux in larvae reared in both 2% (P-value < 0.05) and 50% (P-value < 0.01) ASW, whereas it significantly increased non-DAR proton influx in larvae reared in both 2% (P-value < 0.001) and 50% (P-value < 0.01) ASW. The effect of methazolamide on proton flux in the non-DAR cells differed significantly between larvae reared in 2% and 50% ASW (P-value < 0.001). This effect also differed significantly between the DAR and non-DAR cells in both rearing conditions (P-values indicated in Fig. 3).

DIDS at a concentration of 10^{-6} mol L^{-1} significantly decreased DAR cell proton efflux in larvae reared in 2% ASW (P-value < 0.01), whereas this inhibitor significantly increased DAR cell proton efflux in larvae reared in 50% ASW (P-value < 0.05). DIDS significantly increased non-DAR cell proton influx in larvae reared in both 2% (P-value < 0.01) and 50% (P-value < 0.05) ASW. The effect of DIDS on proton flux in the non-DAR cells differed significantly between larvae reared in 2% and 50% ASW (P-value < 0.001). Additionally, the effect of DIDS on the non-DAR cells of larvae reared in 50% ASW differed significantly (P-value < 0.001) from that of the DAR cells of larvae reared in both 2% ASW and 50% ASW. No significant effects were detected using 0.1% DMSO.

It was noted that in one or more cases, each inhibitor (concanamycin A, methazolamide, DIDS) caused the reversal of flux, in which treatment resulted in a proton efflux becoming an influx. No instances were observed where treatment resulted in a proton influx becoming an efflux.

4. Discussion

The recta of anopheline larvae are distinct from culicine larvae in several ways (Bradley 1987a; Bradley 1994; Smith et al. 2008), yet have only recently been characterized in some detail (Smith et al. 2008). Here we extend that characterization to include structural, physiological, and pharmacological analyses. We gain insight into functional characteristics of the anopheline DAR and non-DAR cells by measuring proton flux at the basal membrane of recta from 2%- and 50%-ASW-reared *An. albimanus* larvae using ISMs. A large proton efflux was measured from the DAR cells into the hemolymph; this contrasted with the flux measured in the non-DAR cells which diminished drastically, often becoming an influx. This proton flux was shown to be independent of rearing salinity in both DAR and non-DAR cells and mediated in part by the actions of V-ATPase, CA and anion exchange. Here we have

combined proton flux data with that of pharmacological inhibition in each region of the anopheline rectum to generate a putative model of ion regulation (Fig. 4) which will be discussed in more detail in the following sections.

4. 1. DAR and non-DAR differ in cell structure

Histological and cytological analyses of freshwater-reared *An. gambiae* and *An. albimanus* suggest that the DAR and non-DAR cells of anopheline larvae differ in cell structure, most notably in the elaboration of the apical membrane. Whereas the DAR cells appear to have very short apical lamellae, elaborate lamellae are evident in the non-DAR cells. This is similar to the cytological differences seen between the AR and PR of saline-tolerant larval culicine recta (Meredith and Phillips, 1973).

Apical lamellae greatly increase the surface area of a membrane, and their presence suggests that the membrane is heavily involved in transport processes. Based on their extensive apical lamellae, the non-DAR cells may be the primary cell type responsible for ion exchange in the rectum as predicted. The DAR cells, like the AR of culicines, may be less involved in ion transport across the apical membrane, and may play more of a role in transport at the basal membrane than the non-DAR cells.

4.2. Several proteins contribute to the proton flux

Several cases were noted in which treatment with an inhibitor caused a proton efflux at the DAR cell membrane to reverse, resulting in a measured proton influx. These results support the idea that the measured fluxes are not the product of a single proton source, but the net result of different transporting proteins, likely generating numerous proton effluxes and influxes at the basal membrane. The large fluxes measured at the DAR cell membrane are therefore a net result of an excess of proton efflux into the hemolymph over proton influx into the cell. Likewise, it is likely that the low effluxes/influxes measured in the non-DAR cells are the result of relatively equal numbers of H^+ being translocated into the hemolymph as there are into these cells.

4.3. Pharmacology

Although proton flux at the basal membrane of the rectum did not measurably differ between larvae reared in 2% and 50% ASW, the effects of specific pharmacological inhibitors on that flux indicate functional differences between the recta of larvae reared in different salinities (Figure 3).

4.3.1. Concanamycin A: V-ATPase inhibitor—Concanamycin A is a membrane permeable macrolide antibiotic that specifically inhibits V-type H^+-ATPase-mediated proton movement (Huss et al. 2002). The V-ATPase is a proton pump and well known membrane energizer important for ion regulation (e. g. Wieczorek et al. 1990). Treatment of DAR cells with concanamycin A resulted in a significant decrease in proton efflux in larvae reared in both 2% and 50% ASW. This suggests the presence of a V-ATPase on the basal membrane of the DAR cells pumping protons into the unstirred layer of the hemolymph. Apparent cytoplasmic localization of a V-ATPase was observed in the DAR cells of both *An. gambiae* and *An. albimanus* using immunohistochemistry (Smith et al. 2008) and it was suggested that the protein may in fact localize to the basal membrane. We have shown the basal membrane of DAR cells to possess an extensive basal labyrinth which extends throughout the majority of the cell. V-ATPase protein distributed on the basal membrane may appear cytoplasmic due to the pervasive and elaborate nature of the membrane.

Treatment of non-DAR cells with concanamycin A had no significant effect on proton influx in 2% ASW-reared larvae, and resulted in a slight, but non-significant, decrease in proton influx

in 50% ASW-reared larvae. This suggests the absence of V-ATPase protein in the non-DAR cells of larvae reared in 2% and 50% ASW; however, V-ATPase has been shown to localize to the apical membrane of the non-DAR cells in larvae reared in both conditions (Okech et al. 2008; Smith et al. 2008). It is possible that Concanamycin A did not effectively permeate the membrane to act on the apically localized protein or that inhibition of an apical V-ATPase does not significantly affect proton flux at the basal membrane, perhaps due to a compensatory proton transporter.

The effect of Concanamycin A on the non-DAR cells of larvae reared in 2% ASW, but not 50% ASW differed significantly from that on the DAR cells of larvae reared in both 2% and 50% ASW. This suggests a functional difference between the non-DAR cells of larvae reared in 50% and 2% ASW. This difference in pharmacological inhibition could be explained by the differential distribution of another proton transporter such as a sodium-hydrogen exchanger (NHE).

In most cases, insect NHEs mediate the electroneutral exchange of intracellular sodium for extracellular protons (Beyenbach 1995; Maddrell and O'Donnell 1992). However, there is evidence that they can also function in the opposite direction (Pullikuth et al. 2006), exchanging extracellular sodium for intracellular protons, similar to mammalian NHEs (Orlowski and Grinstein 2004). Two NHEs have been cloned from *Ae. aegypti* and localized to the recta of larvae (Pullikuth et al. 2006) and adults (Kang'ethe et al. 2007). A similar NHE may provide an additional means of apical proton transport from An. albimanus non-DAR cells into the lumen, thereby compensating for the inhibition of an apical V-ATPase.

4.3.2. Methazolamide: carbonic anhydrase inhibitor—Methazolamide is a specific inhibitor of α-CAs, one isoform of which (AgCA9) we have previously identified as a reliable marker for DAR cells (Smith, K. E. et al. 2007; Smith et al. 2008). Additionally, the mRNA of least two other α-CA isoforms and one β-CA isoform is present in whole recta samples of freshwater-reared *An. gambiae* larvae: AgCA3, a cytoplasmic CA, AgCA6, a secreted CA, and AgCAb, a β-CA against which methazolamide is ineffective (K. E. Smith unpublished data). Both α- and β-CA isoforms catalyze the conversion of cellular CO_2 to HCO_3^- and H^+.

Treatment with methazolamide resulted in a significant decrease in DAR cell proton efflux and a significant increase in non-DAR cell proton influx in larvae reared in both 2% and 50% ASW. CA protein is present in the cytoplasm of the DAR cells (Smith, K. E. et al., 2007). However, these data suggest that CA(s) also influence proton flux in the non-DAR cells, either through the indirect involvement of DAR cell CA(s), or through the presence of an extracellular or cytoplasmic CA isoform associated with the non-DAR cells.

The significant difference in methazolamide action between the DAR and non-DAR cells in both rearing conditions is to be expected despite the prediction of a CA in both cell types. The protons generated by the CA-mediated reaction are likely involved in different transport systems in each cell type, therefore influencing the proton flux in fundamentally different ways. Likewise, the significant difference in methazolamide action in the non-DAR cells between larvae reared in 2% and 50% ASW is likely due to the differential distribution or function of another proton transporter, such as the predicted NHE, and the role it plays on transporting protons generated from the CA-mediated reaction.

4.3.3. DIDS: anion exchange inhibitor—DIDS is a specific inhibitor of cellular anion exchange and is effective against multiple proteins including Na^+-driven and Na^+-independent HCO_3^-/Cl^- transporters and Na^+/HCO_3^- co-transporter as well as Cl^- channels (Grassl & Aronson 1986; Helbig et al. 1988; Boron 2001; Matulef and Maduke 2005). Treatment with DIDS significantly decreased DAR cell proton efflux in 2%-reared larvae, while significantly

increasing DAR cell proton efflux in 50%-reared larvae. This suggests a difference in the functional distribution of HCO_3^- or Cl^--transporting proteins in the DAR cells of larvae reared in 2% versus 50% ASW. Treatment of non-DAR cells with DIDS significantly increased proton influx in larvae reared in both 2% and 50% ASW, although to a significantly greater extent in 50% ASW, supporting the notion of a functional difference in the non-DAR cells of larvae reared at different salinities.

Three HCO_3^- transporting proteins belonging to the SLC4 family (Romero et al., 2004) are predicted to be expressed from the *An. gambiae* genome data; the mRNA of only one of these proteins, AgAE1, is abundantly expressed in the hindgut (Malpighian tubules and rectum) as measured by micro-array and quantitative-PCR (Neira et al. 2008; M. V. Neira personal communication). HCO_3^- transporting proteins are often co-localized with CAs to facilitate the transport out of the cell of HCO_3^- produced by the CA-catalyzed reaction (McMurtrie et al 2004; Sterling et al 2001). As mosquito larvae are thought to excrete HCO_3^- from the rectum, we predict AgAE1 to localize to the apical membrane, transporting HCO_3^- from the cells into the lumen of the rectum. Due to the wide range of proteins inhibited by DIDS, we cannot draw any other specific conclusions regarding our model of ion transport except to say that the results strongly suggest that DIDS-sensitive anion exchange protein activity changes in the DAR and non-DAR cells depending on the salinity of rearing water.

4.4. Putative model for ion transport in the anopheline rectum

We have generated a putative model for ion transport in the larval rectum of anopheline mosquitoes (Fig. 4) based on current physiological and pharmacological data as well as previous immunohistochemical data (Rheault et al. 2007;Okech et al. 2008;Smith et al. 2008). This model supports the hypothesis that the primary function of the non-DAR cells changes in response to the ionic needs of the larvae. Anophelines reared in fresh water actively resorb ions via their rectum to maintain constant ionic and osmotic hemolymph concentrations (Bradley, 1994). By contrast, anophelines reared in saline water must excrete the excess ions ingested while feeding via rectal production of a hyperosmotic urine. Based on our model, a potential mechanism for Na^+ resorption is evident in the non-DAR cells of 2% ASW-reared larvae, whereby Na^+ is transported from the lumen in to the cell via an NHE and is then transported into the hemolymph in exchange for K^+ via a Na^+K^+-ATPase. Basal Na^+K^+-ATPase is considerably down-regulated in the non-DAR cells of larvae reared in 50% ASW (Smith et al. 2008), and we predict that the apical NHE may also be down-regulated in saline conditions. This change in protein distribution would interfere with Na^+ resorption in the non-DAR cells and may indicate a shift in primary rectal function, from resorption in fresh water, to secretion in saline water.

The DAR cells are hypothesized to have a main role in HCO_3^- excretion (Smith et al. 2008). However, this hypothesis is based on the idea that CA exclusively localizes to the DAR cells. As pharmacological data now suggests that CA is present in both DAR and non-DAR cells, it is likely that DAR cells also have a role in basal resorption of essential ions and nutrients from the primary urine, similar to that suggested for the AR of culicine larvae (Meredith and Phillips 1973; Bradley and Phillips 1977).

4.5. Conclusions

We have further characterized the DAR and non-DAR cell types of the anopheline larval rectum, demonstrating that the two cell types differ in basal membrane proton flux, and that V-ATPase, CA, and anion exchanger proteins have a major role in mediating proton flux in both cell types. Additionally, differences in the response of proton flux to inhibitors in larvae reared in 2% versus 50% ASW indicate changes in protein function between the two rearing conditions. Finally, histological analyses suggest that the non-DAR cells are structurally suited

for mediating ion transport. These data support a model of rectal ion regulation in which the non-DAR cells have a resorptive function in freshwater-reared larvae and a secretive function in saline water-reared larvae. In this way, anopheline larvae may adapt to varying salinities.

Ion regulation is a biological process crucial to the survival of mosquito larvae. The ability to shift protein distribution, thereby altering cell function, affords larvae the ability to survive and flourish in a wider range of habitats. This work has begun to characterize the function of the anopheline rectum as it relates to adaptation and ion regulation. Future work describing the transport of other ions including K^+, Cl^-, and Na^+ within the rectal cells is needed to enhance this model of ion transport and further our understanding of rectal function. Only through full comprehension of the proteins involved in, and the mechanisms responsible for these adaptive abilities can we take advantage of this vital process for the development of vector control.

Acknowledgments

This research was supported in part by grants through the National Institute of Health: NIAID AI-45098-10 (P. J. Linser), P41 Rr01395 (P.J.S. Smith), and an NSF research experience for undergraduates (REU) grant to the University of Florida Whitney Laboratory: award # 0648969. S.L. Raymond and M.L. Valenti were supported by and award from the HHMI Science for Life education program at the University of Florida. We graciously thank M. Messerli for his time, expertise, and instruction on the construction and use of the ISMs.

Abbreviations

AR	Anterior rectum
ASW	Artificial sea water
CA	Carbonic anhydrase
DAR	Dorsal anterior rectum
DIDS	4,4′-Diisothiocyanatostilbene-2,2′-disulfonic acid Disodium salt
H^+	Protons
ISM	Ion selective microelectrode
J	Flux
NHE	Sodium hydrogen exchanger
PR	Posterior rectum
TEM	Transmission electron microscope

References

Beyenbach KW. Mechanism and regulation of electrolyte transport in Malpighian tubules. J Insect Physiol 1995;4:197–207.

Boron WF. Sodium-coupled bicarbonate transporters. JOP 2001;2:176–181. [PubMed: 11875256]

Bradley TJ. Evidence for hypo- and hyperosmotic regulation in the larvae of an anopheline mosquito. Am Zool 1987a;27(4):30A.

Bradley TJ. Physiology of osmoregulation in mosquitoes. Annu Rev Entomol 1987b;32:439–462. [PubMed: 2880552]

Bradley, TJ. The role of physiological capacity, morphology, and phylogeny in determining habitat use in mosquitoes. In: Wainwright, PC.; Reilly, SM., editors. Ecological Morphology. The University of Chicago Press; Chicago and London: 1994. p. 303-318.

Bradley TJ, Phillips JE. The location and mechanism of hyperosmotic fluid secretion in the rectum of the saline-water mosquito larvae*Aedes taeniorhynchus*. J Exp Biol 1977;66:111–126. [PubMed: 858991]

Clark TM, Koch A, Moffet DF. The anterior and posterior 'stomach' regions of larval *Aedes aegypti* midgut: regional specialization of ion transport and stimulation by 5-hydroxytryptamine. J Exp Biol 1999;202:247–252. [PubMed: 9882637]

Grassl SM, Aronson PS. Na+/HCO3-co-transport in basolateral membrane vesicles isolated from rabbit renal cortex. J Biol Chem 1986;261(19):8778–83. [PubMed: 3013862]

Harvey WR, Nedergaard S. Sodium-independent active transport of potassium in the isolated midgut of the cecropia silkworm. P Natl Acad Sci USA 1964;51:757–65.

Helbig H, Korbmacher C, Kühner D, Berweck S, Wiederholt M. Characterization of Cl-/HCO3- exchange in cultured bovine pigmented ciliary epithelium. Exp Eye Res 1988;47(4):515–23. [PubMed: 3181332]

Huss M, Ingenhorst G, König S, Gabel M, Dröse S, Zeeck A, Altendorf K, Weiczorek H. Concanamycin A, the specific inhibitor of V-ATPases, binds to the V_o subunit c. J Biol Chem 2002;277(43):40544–40548. [PubMed: 12186879]

Kang'ethe W, Aimanova KG, Pullikuth AK, Gill SS. NHE8 mediates amiloride-sensitive Na+/H+ exchange across mosquito Malpighian tubules and catalyzes Na+ and K+ transport in reconstituted proteoliposomes. Am J Physiol Renal Physiol 2007;292(5):F1501–12. [PubMed: 17287198]

Maddrell SH, O'Donnell MJ. Insect Malpighian tubules: V-ATPase action in ion and fluid transport. J Exp Biol 1994;172(Pt 1):417–429. [PubMed: 9874752]

Matulef K, Maduke M. Side-dependent inhibition of a prokaryotic ClC by DIDS. Biophys 2005;89:1721–1730.

McMurtrie HL, Cleary HJ, Alvarez BV, Loiselle FB, Sterling D, Morgan PE, Johnson DE, Casey JR. The bicarbonate transport metabolon. J Enzyme Inhib Med Chem 2004;19(3):231–6. [PubMed: 15499994]

Meredith J, Phillips JE. Rectal ultrastructure in salt- and freshwater mosquito larvae in relation to physiological state. Z Zellforsch 1973;138:1–22. [PubMed: 4348887]

Messerli, MA.; Robinson, KR.; Smith, PJS. Electrochemical sensor applications to the study of molecular physiology and analyte flux in plants. In: Volkov, AG., editor. Plant electrophysiology - Theory and Methods. Springer; New York: 2006. p. 73-108.

Neira Oviedo M, VanEkeris L, Corena-Mcleod MDP, Linser PJ. A microarray-based analysis of transcriptional compartmentalization in the alimentary canal of *Anopheles gambiae* (Diptera: Culicidae) larvae. Insect Mol Biol 2008;17:61–72. [PubMed: 18237285]

Okech BA, Boudko DY, Linser PJ, Harvey WR. Cationic pathway of pH regulation in larvae of *Anopheles gambiae*. J Exp Biol 2008;211:957–968. [PubMed: 18310121]

Orlowski J, Grinstein S. Diversity of the mammalian sodium/proton exchanger SLC9 gene family. Pflugers Arch 2004;447(5):549–65. [PubMed: 12845533]

Padan E, Venturi M, Gerchman Y, Dover N. Na(+)/H(+) antiporters. Biochim Biophys Acta 2001;1505 (1):144–57. [PubMed: 11248196]

Pullikuth AK, Aimanova K, Kang'ethe W, Sanders HR, Gill SS. Molecular characterization of sodium/proton exchanger 3 (NHE3) from the yellow fever vector, *Aedes aegypti*. J Exp Biol 2006;209(Pt 18):3529–44. [PubMed: 16943493]

Rheault MR, Okech BA, Keen SBW, Miller MM, Meleshkevitch EA, Linser PJ, Boudko DY, Harvey WR. Molecular cloning, phylogeny and localization of AgNHA1: the first Na^+/H^+ antiporter (NHA) from a metazoan, *Anopheles gambiae*. J Exp Biol 2007;210:3848–3861. [PubMed: 17951426]

Richards R, Linser P, Armentrout RW. Kinetics of the assembly of a parvovirus, minute virus of mice, in synchronized rat brain cells. J Virol 1977;22:778–793. [PubMed: 559779]

Romero MF, Fulton CM, Boron WF. The SLC4 family of HCO 3 - transporters. Pflugers Arch 2004;447 (5):495–509. [PubMed: 14722772]

Sachs J, Malaney P. The economic and social burden of malaria. Nature 2002;415:680–685. [PubMed: 11832956]

Smith KE, VanEkeris LA, Linser PJ. Cloning and characterization of AgCA9, a novel α-carbonic anhydrase from *Anopheles gambiae* Giles sensu stricto (Diptera: Culicidae) larvae. J Exp Biol 2007;210:3919–3930. [PubMed: 17981859]

Smith KE, VanEkeris LA, Okech BA, Harvey WH, Linser PJ. Larval anopheline mosquito recta exhibit a dramatic change in localization patterns of ion transport proteins in response to shifting salinity: a

comparison between anopheline and culicine larvae. J Exp Biol 2008;211(Pt 19):3067–3076. [PubMed: 18805805]

Smith PJS, Hammar K, Porterfield DM, Sanger RH, Trimarchi JR. Self-referencing, non-invasive, ion selective electrode for single cell detection of trans-plasma membrane calcium flux. Microsc Res Techniq 1999;46:398–417.

Smith, PJS.; Sanger, RS.; Messerli, MA. Principles, development and applications of self-referencing electrochemical microelectrodes to the determination of fluxes at cell membranes. In: Michael, AC., editor. Methods and new frontiers in neuroscience. CRC Press; Boca Raton: 2007. p. 373-405.

Sterling D, Reithmeier RA, Casey JR. A transport metabolon Functional interaction of carbonic anhydrase II and chloride/bicarbonate exchangers. J Biol Chem 2001;276:47886–47894. [PubMed: 11606574]

The World Health Report 1996 fighting disease, fostering development. Geneva: World Health Organization; 1996. p. 46

Wieczorek H, Cioffi M, Klein U, Harvey WR, Schweikl H, Wolfersberger MG. Isolation of goblet cell apical membrane from tobacco hornworm midgut and purification of its vacuolar-type ATPase. Meths Enzymol 1990;192:608–616.

Wieczorek H, Putzenlechner M, Zeiske W, Klein U. A vacuolar-type proton pump energizes K^+/H^+ antiport in an animal plasma membrane. J Biol Chem 1991;266:15340–7. [PubMed: 1831202]

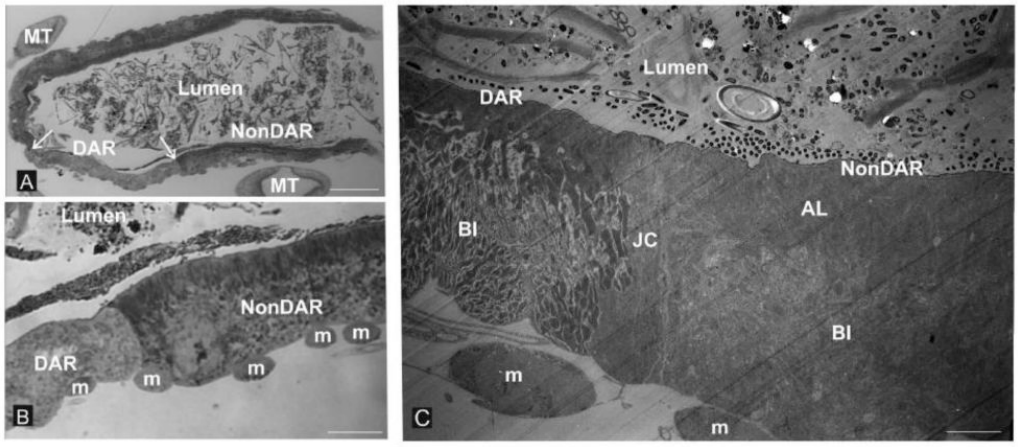

Figure 1.

Rectal cytology. The rectal cells of freshwater-reared *An. gambiae* larvae are lined on the luminal (apical) side by cuticle and on the hemolymph barrier (basal) side by circumferential muscles. Two cell types are distinguishable by the presence or absence of a prominent apical border of apical lamellae (AL, panels "B" and "C"). Panel "A" shows relatively low magnification and the disposition of the DAR and nonDAR cells relative to the borders between the two cell types (arrows) in the anterior region of the rectum and the surrounding profiles of Malpighian tubules (MT). Panel "B" is a higher magnification of the boundary of the two cell types with the basal array of muscle fiber bundles (m) indicated. Note the clear distinction in appearance of the DAR and non-DAR cells at the luminal (apical) surface. Panel "C" shows a transmission electron micrograph of the DAR-nonDAR junction depicting the disparity in the organization of the two cell types. Also evident is a third cell type which is a junctional cell (JC) wich separates the DAR and non DAR cells. Also note that the appearance of the elaboration of basal membranes known as the basal infoldings (BI) is distinct between the DAR and nonDAR cells. Circumferential muscle fiber bundles at the basal extreme (m) are also evident. Magnification bars: "A" = 50 μm; "B" = 12.5 μm; "C" = 3.6 μm.

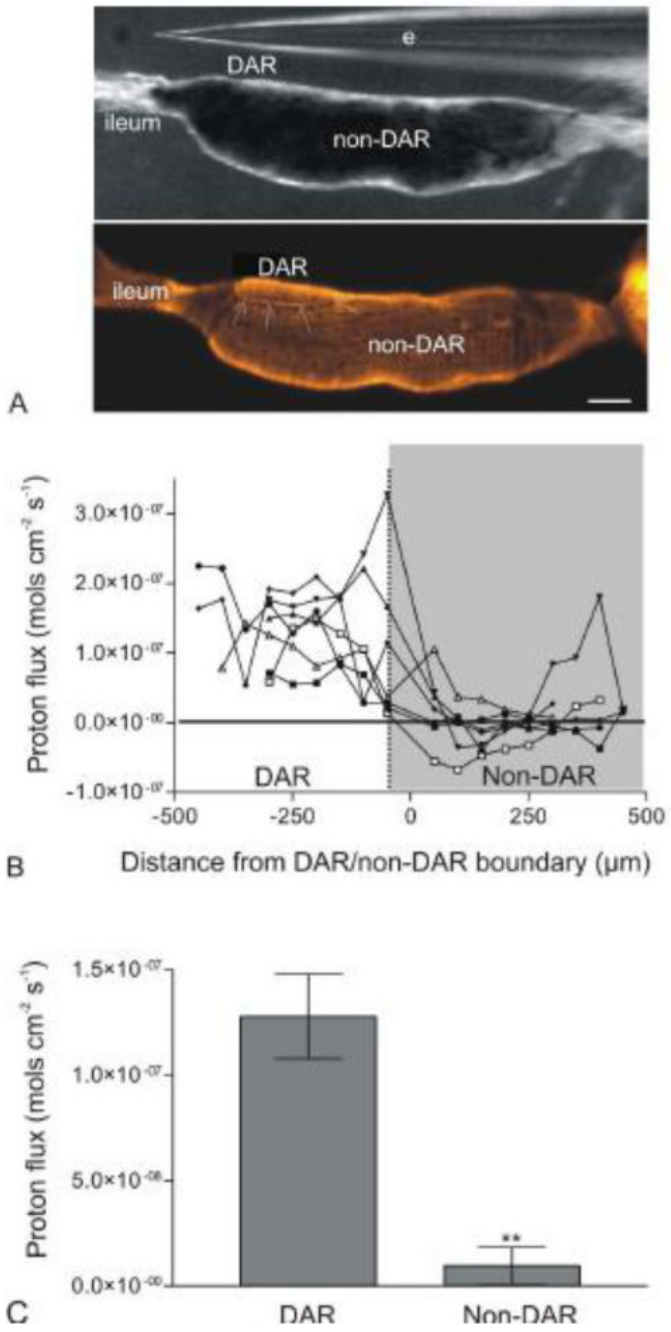

Figure 2.

Measure of proton flux at the basal membrane of the DAR and non-DAR cells of *An. albimanus* larvae using ISMs in a self-referencing mode. (A) Image illustrating the larval rectum under a light microscope during proton flux measurements (top panel), and post-stained with rhodamine 123 to visualize the DAR/non-DAR boundary (arrows; bottom panel). (B) Proton flux measurements for seven individual preparations (three larvae reared in 2% ASW and four larvae reared in 50% ASW) beginning at the rectum-ileum junction and continuing in 50µm intervals until the end of the rectal cells. Each data point represents an average of continuous measurements taken over a five minute period. There was a consistent, large proton efflux in the area of the DAR cells in all preparations. This efflux dropped drastically, often

becoming an influx at the non-DAR cells. (C) Averaged DAR and non-DAR proton flux measurements of the same seven larvae represented in (B). Error bars indicate standard error of the mean. Difference in proton flux between the DAR and non-DAR cells was statistically significant (P-value < 0.01) as determined using a paired t-test and reported as a two-tailed P-value. Scale bar: 100μm. e: electrode. □, ●, ○: larvae reared in 2% ASW; ◆, ▼, ▲, ■: larvae reared in 50% ASW.

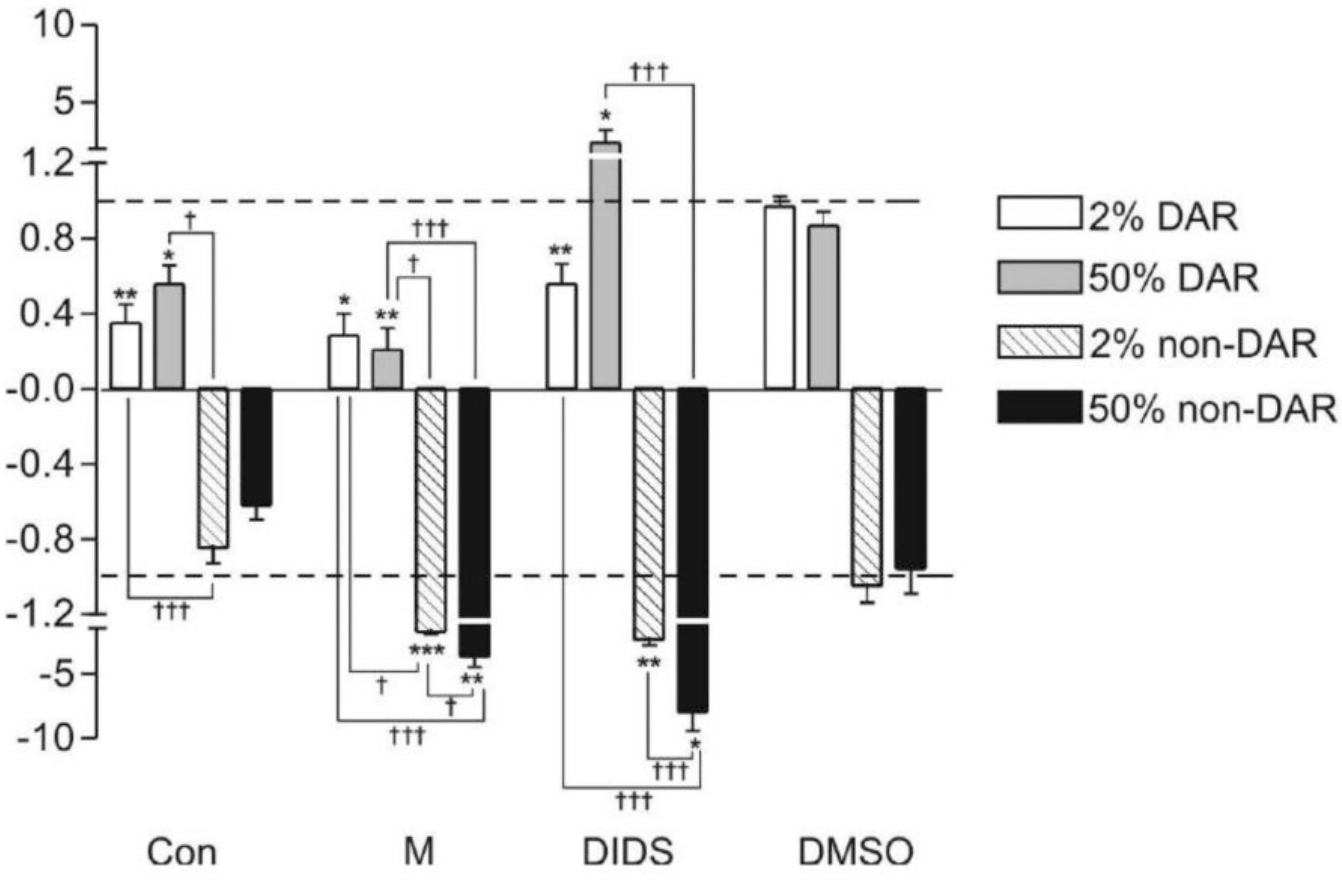

Figure 3.

Pharmacological inhibition of proton flux at the basal membrane of 2% and 50% ASW-reared *An. albimanus* rectum. Y-axis indicates ratio of flux after treatment, to flux before treatment with an inhibitor. A value of "1" (for efflux) or "-1" (for influx) indicates no change in flux and is indicated by a dashed line. Inhibitors included a V-ATPase inhibitor, concanamycin A (Con; 10^{-6} mol L^{-1}), a carbonic anhydrase inhibitor, methazolamide (M; 10^{-4} mol L^{-1}), and an anion exchange inhibitor, DIDS (10^{-6} mol L^{-1}), as well as a DMSO (10^{-6} mol L^{-1}) vehicle control. All results represent an average of n > 5 preparations. Significance asterisks: * = P-value < 0.05; ** = P-value < 0.01; *** = P-value < 0.005. Asterisks represent significance of flux before, to flux after inhibitor for each individual preparation. Significance daggers: † = P-value < 0.05; ††= P-value < 0.01; ††† = P-value < 0.001. Daggers represent significance of flux inhibition between cell types and rearing conditions for each inhibitor.

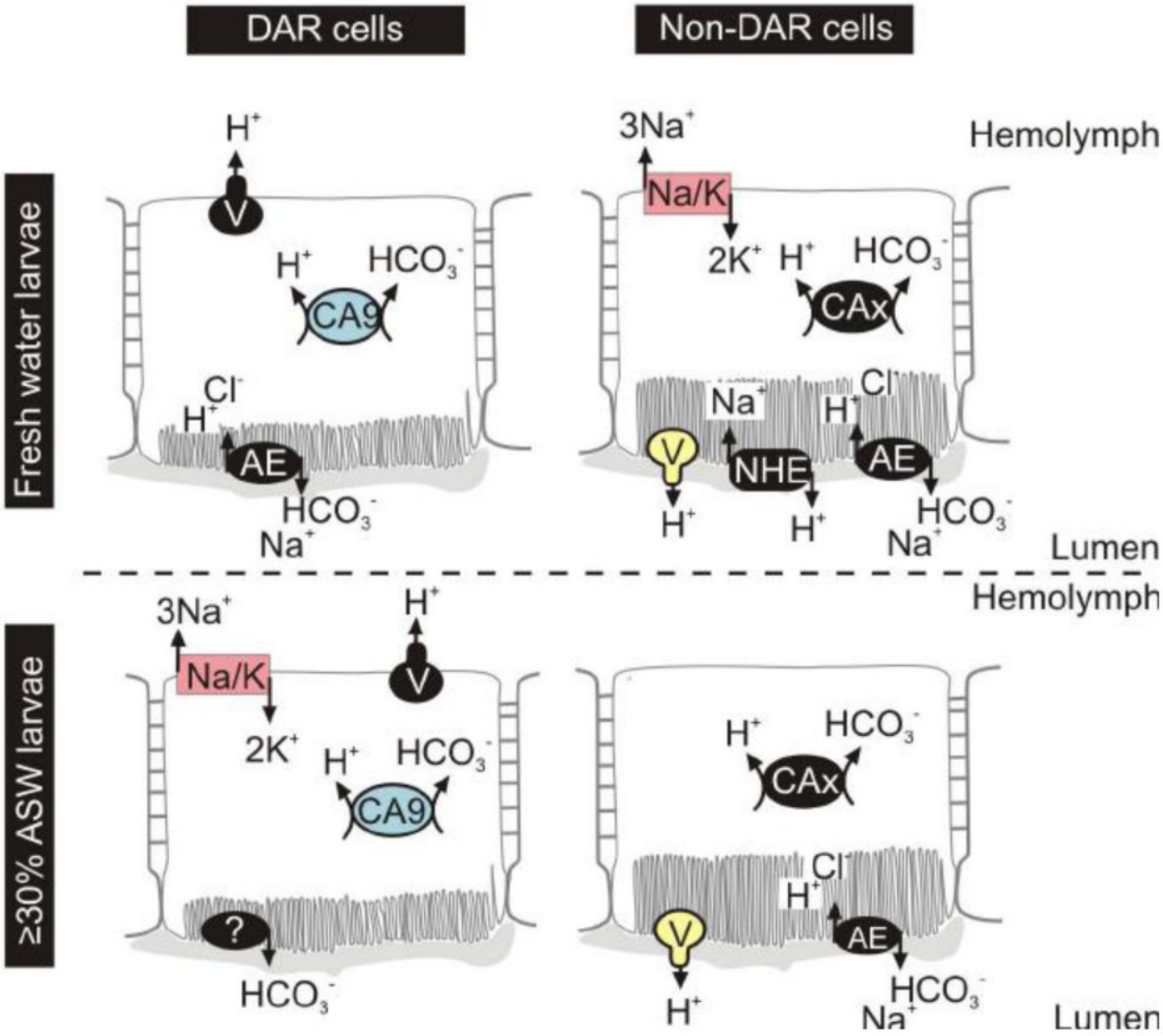

Figure 4.

Putative model for ion transport in the anopheline rectum of larvae reared in fresh or saline water. Proteins in color have been previously immunolocalized, whereas proteins in black are predicted. AE: anion exchanger; CA: carbonic anhydrase; Na/K: sodium/potassium ATPase; NHE: sodium/hydrogen exchanger; V: V-ATPase.